Electronic Supplementary Material (ESI) for Lab on a Chip.

Supporting Information for

High-precision modular microfluidics by micromilling of interlocking injection-molded blocks

Crystal E. Owens and A. John Hart*

Department of Mechanical Engineering and Laboratory for Manufacturing and Productivity, Massachusetts Institute of Technology, 77 Massachusetts Avenue, Cambridge, Massachusetts 02139, USA

***Corresponding Author:** *E-mail:* ajhart@mit.edu

Video Descriptions

SI Video 1. A video of system assembly shows the creation of a series of systems from bricks. The working fluid is water with food coloring of various colors.

SI Video 2. A video of system fabrication shows the micromilling and tape sealing of a single brick unit for mixing fluids.

Design File Descriptions

Design Files 1. A set of .prn files for creating the droplet generating brick shown in Fig 1 and Fig 6, for use on a Roland SRM-20 micromill and a PMT square endmill with diameter 0.0190". The (0,0) position is set as the bottom left corner of the front face of the brick.

Design Files 2. A set of .prn files for creating a brick with a straight channel, for use on a Roland SRM-20 micromill and a PMT square endmill with diameter 0.0190". The (0,0) position is set as the bottom left corner of the front face of the brick.

Design Files 3, 4. Two .stl files for creating the system (3) inlet and (4) outlet bricks shown in Fig 7, optimized for printing via SLA on a Formlabs Form2 with Clear resin.

Design Files 5, 6. Two .stl files for creating the camera mount structures shown in Fig 7 and SI Fig 13, optimized for printing via FDM on a Stratasys Mojo with ABS plastic.

Design Files 7-8. .sldprt files for an assortment of bricks shown in Fig 1.

Comparison of fabrication methods

To select the method for modifying LEGO bricks with microfluidic pathways, we compared (SI Table 1) laser ablation, hot embossing, milling, and stereolithography onto brick surfaces qualitatively according to several performance attributes.

SI Table 1 Methods to create channels on bricks were compared qualitatively. Micromilling was selected for its combination of speed, precision, and serial nature.

○ Poor ◐ Good ● Great	Laser ablation	Hot embossing	Milling	SLA
Processing speed	○	●	◐	◐
Feature resolution	●	Based on master	●	●
Ability to customize each piece	●	○	●	●
Material compatibility	◐	○	●	○
Surface roughness	●	Based on master	●	●
Infrastructure needs	◐	◐	●	●

In addition, costs are calculated per unit for each brick, as the fractional cost of the brick ($0.05-0.07), the sealing film ($0.05), and the o-ring ($0.04). Cost per lithographic chip varies widely, and was estimated from several articles and sites including http://ufluidix.com/pricing/.

Typical milling parameters for fabrication of fluidic bricks

Milling parameters were suggested by software (GWizard, CNCCookbook), and refined by experiments to reduce tool breakage and surface roughness (Fig 2; Table 2, on the low end for micromilling).

SI Table 2 Typical cutting parameters used in micromilling here, for 9500 revolutions per minute and 2 flutes: tool diameter, feed, depth of cut material removal rate (MRR), cutting velocity (Vc), and chip load (feed per cut).

Tool diameter		Feed (mm/min)		Depth	MRR (mm^3/min)		Vc		Chip load
(in)	(mm)	ABS	PC	(mm)	ABS	PC	(mm/min)	(m/s)	(mm^3/rev)
0.0040	0.102	50	30	0.03	0.2	0.1	3030	0.05	8.0 E-06
0.0070	0.178	90	60	0.04	0.6	0.4	5300	0.09	33.6 E-06
0.0100	0.254	120	90	0.06	1.8	1.4	7580	0.13	96.2 E-06
0.0190	0.483	270	190	0.12	15.6	11.0	14400	0.24	822.9 E-06

Sizing of apertures in fluidic bricks

Using a balance of capillary and gravitational forces ($\frac{2\sigma}{R} = \rho g h$), apertures were sized such that capillary pressure retained water inside when a brick was detached from a system and apertures were exposed to air (SI Fig 1).

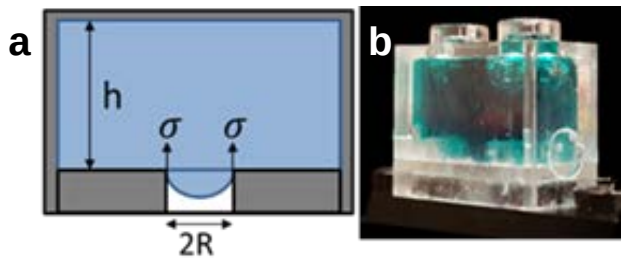

SI Figure 1. Calculation of geometry to retain fluid inside bricks via surface tension. (Right) Demonstration of a brick that was filled to the top with teal fluid when it was in a brick network, and removed to be imaged, without leaking.

Fixturing bricks during milling

During micromilling, bricks were held in place using a LEGO fixture (SI Figure 2) attached to the table of the micromill with double-sided tape; this was possible because of the low cutting forces of micromilling (<5 N). The repeatability of brick mounting made it easy to rotate and reposition blocks to mill on different faces, allowing machining of multiple features on adjacent faces of each brick, including serpentine micromixing channels across corners (SI Fig. 2f).

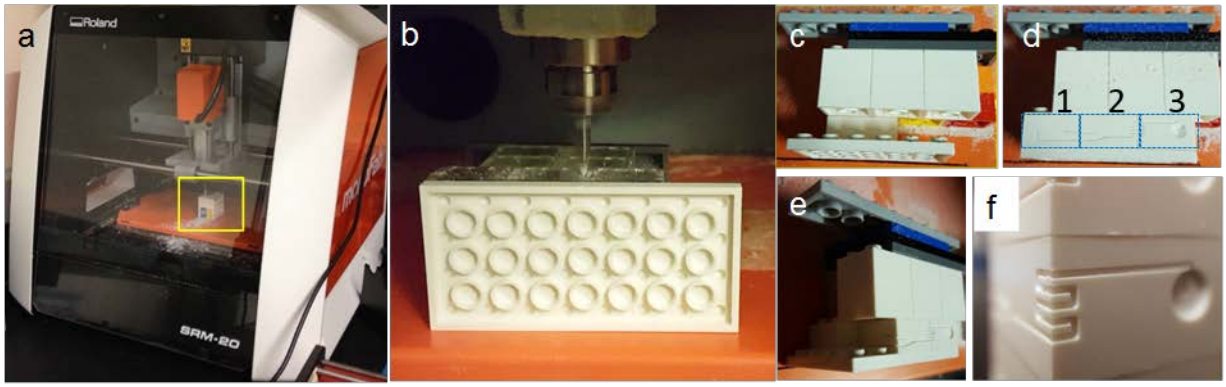

SI Figure 2 Micromilling fixture using LEGO bricks. (a, b) A bottom layer of LEGO bricks was adhered via double-sided tape to the micromill table. The fixture had two supporting layers of 3-4 bricks for stability, and one or more large plate of LEGOs holding the entire fixture the top and bottom surfaces. (c) For geometries that required connected features on more than one face (*i.e.*, all of them), bricks were rotated around the corner of interest, into the adjacent spot on the fixture, instead of being rotated in place, in order to reduce the effect of any angular misalignment of the fixture or mill. For example, the pictured brick would be milled sequentially in spots labeled 1, 2, and 3 to modify each side (d, e) This resulted in well-aligned corner cuts on the shown advective mixing unit.[1]

[1] Incidentally, misaligned corners should improve the mixing ability of the shown brick by introducing more intense geometrical changes, but it is desirable to reduce misalignment where it is due purely to error.

Milled section

A laser-interferometry scan shows the rectangular sidewalls in a brick imaged at an angle and circular corrugations decorating the bottom of the as-milled channel surface (SI Fig 3).

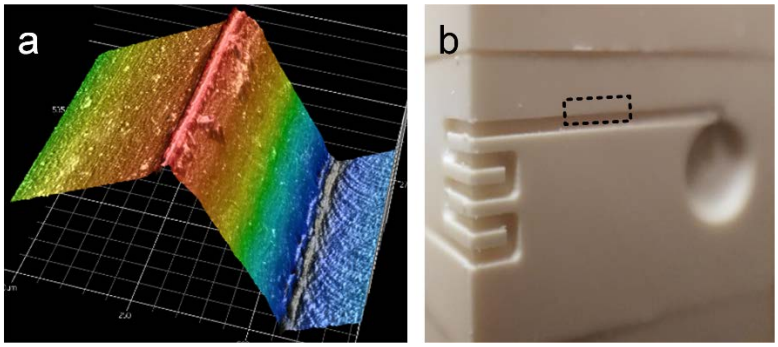

SI Figure 3. (a) A laser-interferometry scan (Keyence VK-X) shows sidewalls in a brick imaged at an angle, with the blue region indicating the base of the channel. The depth of the channel is 420 µm. (b) Picture showing where on a channel the scan was taken.

Interchangeability

In SI Fig. 4, we show the measured data for locating repeatability, variation in width, and unit interchangeability. Interchangeability is defined as the root mean sum in quadrature of the repeatability of location and dimensional variation of a brick width.

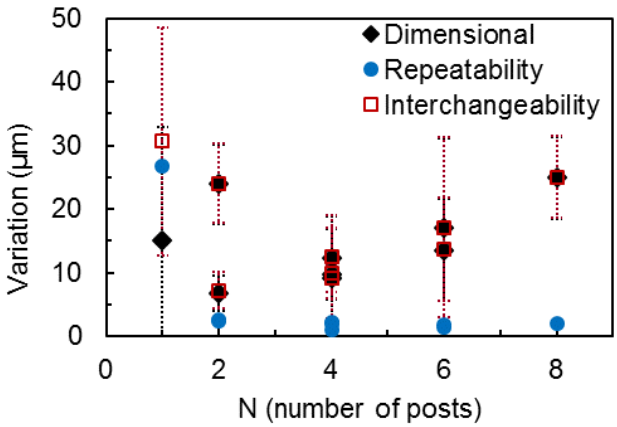

SI Fig 4. Interchangeability (red square), repeatability (blue circle), and dimensional variation of brick widths (black diamond) was measured for a variety of standard sizes. Error bars for dimension and repeatability variation represent one standard deviation in variation calculated for groups of measured bricks, while the square root of the sum of those two errors is represented by the error bar for interchangeability.

Attachment mechanics

Bricks connect to the baseplate via elastically averaged contacts, which causes the bricks to expand elastically by a small amount (<50 µm; SI Fig 4b) when mounted due to the stress exerted by posts on the baseplate, but not enough to completely fill the brick-brick gap. This is verified by by a finite element analysis in SolidWorks (SI Fig 4b).

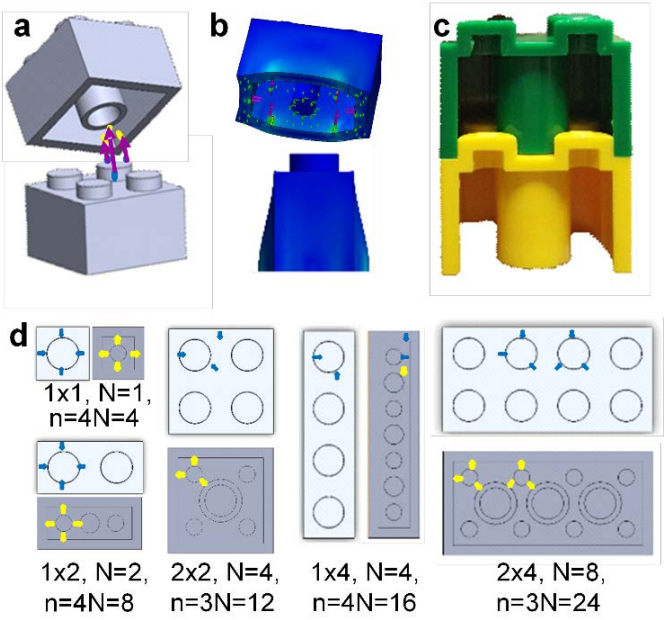

SI Figure 5 Attachment mechanics of LEGO bricks on LEGO baseplates. (a) Bricks attach when a series of posts make contact with the inside of a second brick, exerting force on post and brick walls. (b) Finite element model of a mounted brick showing the resulting deformation (exaggerated scale running from cyan (highest) to blue (none)). Magenta arrows locate the applied force and green objects indicate fixed surfaces. The true scale of maximum deflection is <50 µm per side as measured with a micrometer. The force exerted on the outer walls of the brick by a post was estimated as 10 N using a Hertzian contact stress analysis based on the deformed area of a post attached to a transparent brick. (c) Photograph of two bricks cut in half and attached together, showing both a uniform thickness cross-section and points of contact. (d) Locations of contact points for the five most common bricks, shown on the top (light gray) and bottom (dark gray) brick surfaces, and once for each type of post attachment. Note: (d) was styled after a nicely illustrative figure in [35].

O-ring Measurements

Sealing capacity was calculated versus O-ring compression using data and equations from [37] (SI Fig 6), and verified by experiment to the limit of our testing equipment (SI Fig 7).

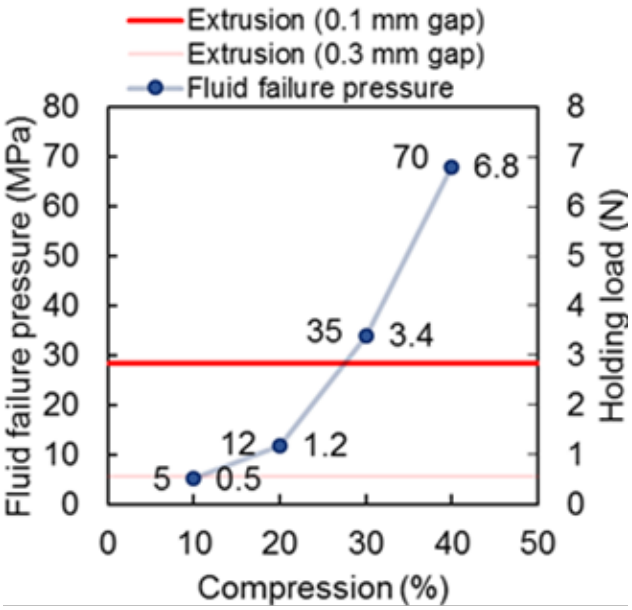

SI Figure 6. Calculations to guide the design of the O-ring seat in a milled brick. The left axis indicates the fluid pressure required to dislodge the O-ring normal to the sealing face, with values calculated based on handbook values for the holding load required for a given compression value (and Pressure = (Holding force)/(O-ring projected area)). Red lines indicate the fluid pressure at which the O-ring seal will fail by material extrusion into the gap, which depends on material, gap size, and fluid pressure, not compression.

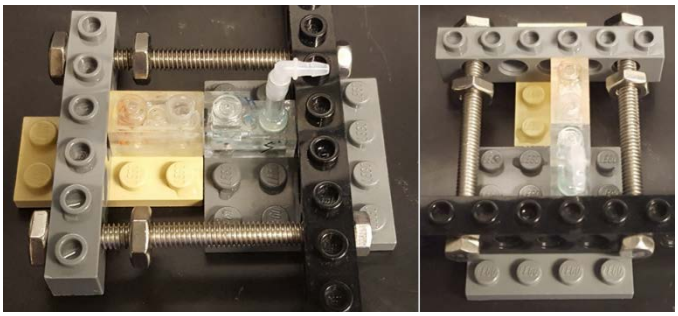

SI Figure 7. Fixture used to vary the spacing between bricks, connected by an O-ring, to measure sealing pressure as a function of O-ring compression. A liquid pressure dial gauge (McMaster-Carr #4026K3) was attached between the right brick and a syringe, and the left brick was closed. Leakage pressure was identified as the maximum reading on the pressure gauge, after which the pressure decreased and fluid emerged.

Effect of corners on fluid flow

A single brick fluidic system having a channel with five additional corners was compared to a straight path to see the effect of corners on the pressure drop within a system (SI Fig 8). This validated that the slightly tortuous geometry required for intra-brick sealing does not have a large impact on the flow inside the system.

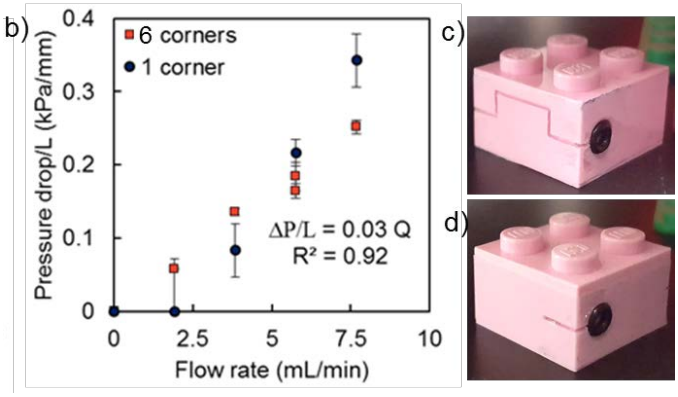

SI Figure 8 (a) Replotting pressure drop versus Reynolds number for experimental and theoretical values for laminar flow suggest effects from inertia and a transition to turbulence or another effect. (b) Two geometries with different numbers of 90 degree corners and dissimilar lengths have indistinguishable pressure drop per length, indicating minimal effects from corners at moderate flow rates. (c,d) Bricks used in the system.

Number of modules in typical microfluidic research systems

We surveyed all articles in the first issue of *Lab on a Chip* published in 2016 and in 2012 and determined the number of procedures that were performed in each device, and therefore how many distinct modules would be necessary in a modular system. We determined that they typically have ~4-8 procedures such as fluid inlet and outlet, testing and incubation chambers, heaters, sensors, and cameras in a complete device (SI Fig 9).[40–59] Therefore, we can conclude that the brick-based modular system could be scaled to accommodate this typical size, and much larger systems.

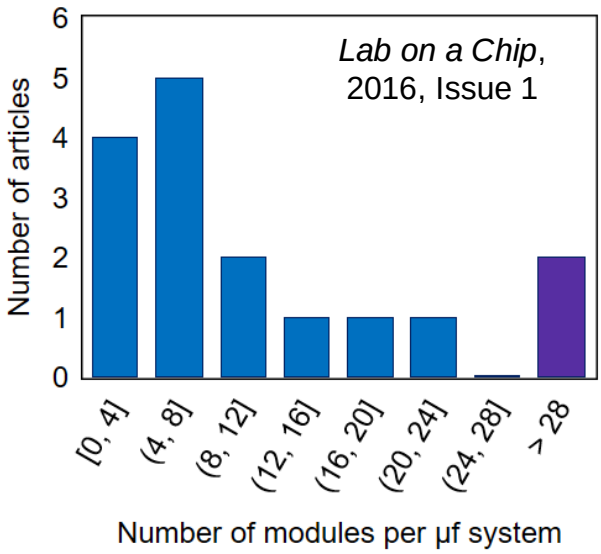

SI Figure 9 Number of functions performed by the microfluidic devices published in *Lab on a Chip*, 2016 and 2012, issues 1, where in an equivalent modular system one could envision decomposing the devices into different bricks. Values greater than 28 are from multiplexed systems with an average value of ~990 modules.

Commercial Glass Chip Incorporation

While our machined modules are useful for interconnection and system creation, it is also beneficial to interface with conventional devices which can have higher performance despite their fabrication cost and complexity. To address this point, we purchased and inserted a glass microfluidic droplet generator into the system, to demonstrate channels of (1) a different material and (2) smaller size than we could make in the regular milled LEGO brick network (SI Fig 10). The incorporation included two inlets and an outlet to the chip, all using o-rings on the machined module side, as well as two positioning blocks (SI Fig 10a, inset) which were milled to position the chip both laterally and maintain an appropriate gap between the bricks and the O-rings for sealing.

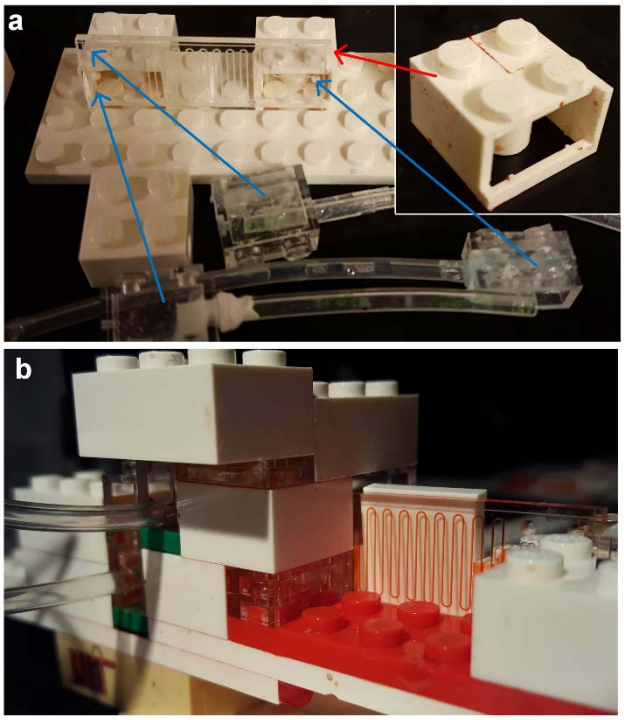

SI Figure 10. (a) Photograph showing microfluidic system incorporating the commercial glass chip, and inset showing regular droplets passing through the chip. (b) image showing fluid flow through the chip.

Orientation in FDM 3D printing

In FDM 3D printing, an object is built by extruding a bead of melted thermoplastic along a path. Due to the finite size of the bead and interlayer adhesion, the orientation of printing has an impact on the shape and mechanical capacity of the final object. We printed LEGO bricks with a variety of orientations and layer heights to determine the optimal process to make repeatable, dimensionally accurate units for modular microfluidics and accessory components. SI Fig 11 shows three key orientations for printing. The middle one (printing vertically, “upside-down”) was chosen because it gave the best dimensional accuracy, including isotropy in brick width being true to size. It also required the least support material, so the walls of the structure were smoother than for other printing orientations. Layers in SLA have a similar appearance, though the typical desired printing orientation is at a skew angle to the build plate, due to viscous forces of the resin on thin printed layers, and the orientation did not have a considerable influence on the dimensions or repeatability.

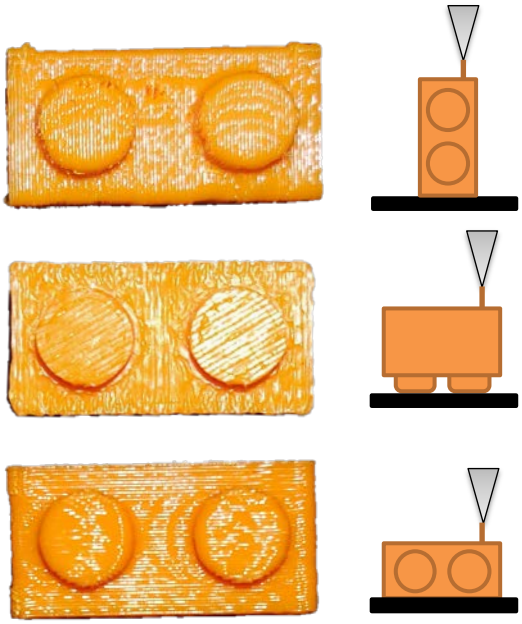

SI Figure 11. Photographs and schematics of FDM printed bricks with a selection of different orientations.

Mechanical Repeatability of 3DP Lego Bricks

Repeatability was measured for FDM and SLA printed bricks as a large number of points, and then position was plotted over time to show there is initial plastic deformation and then a more stable period before final fracture (SI Fig 12). For SLA-printed bricks, characteristics include an initial widely varying initial variation in position, indicating plastic deformation, a narrower range of position with a mean downward drift, and then the brick appears to experience failure after which point variation in position is quite large. Repeatability in SI Fig 12a is indicated for the middle range only. FDM-printed bricks exhibit the same initial change in position, but afterwards mostly converge onto a narrow and consistent distribution (SI Fig 12c). Both types of bricks exhibited permanent deformation, which was absent on standard LEGO bricks even after thousands of trials (SI Fig 12d).

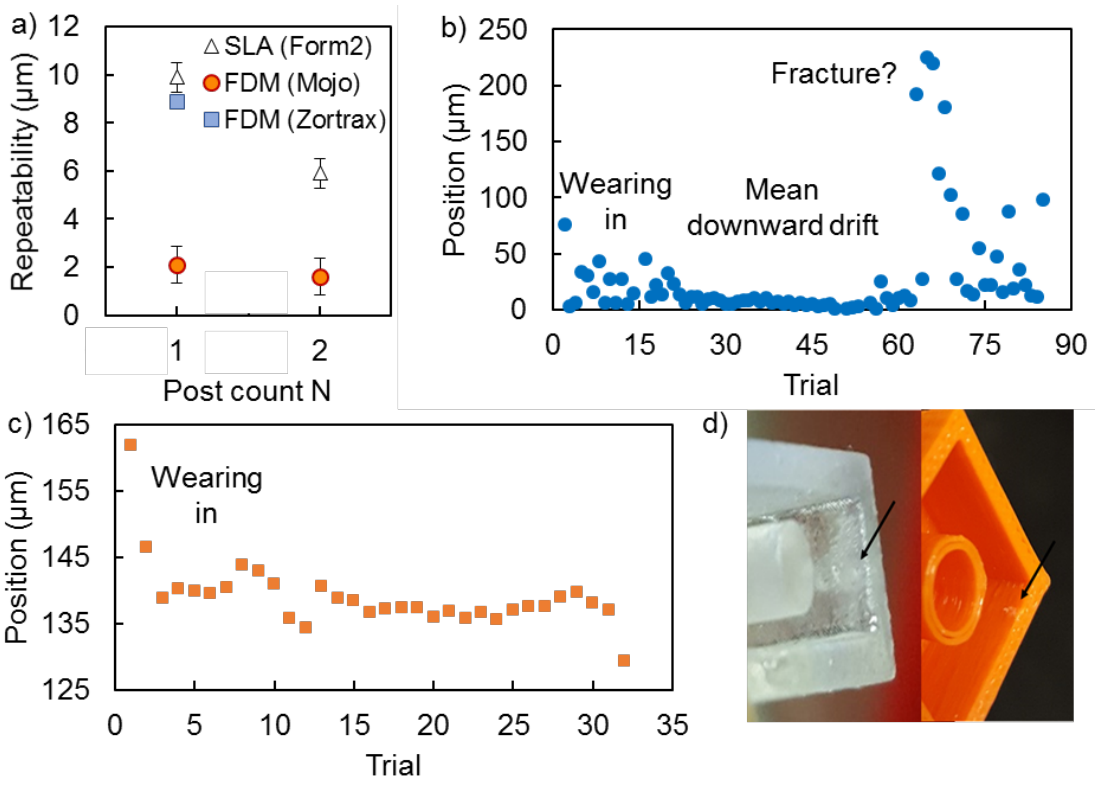

SI Figure 12. Repeatability of 3D-printed bricks when mounted to a standard LEGO brick. (a) Final results show repeatability ranging from 2 to 10 µm for different sizes of the same bricks. Here, unlike before, post count refers to the number of posts orthogonal to the measured edge, instead of complete post count, to observe for effects of printing orientation. Measurements of repeated mountings of the same 3DP bricks on a standard LEGO brick shows systematic effects, plotted for one experiment each for (b) SLA and (C) FDM bricks. (d) After experiments, we observed permanent deformation at the contact points (black arrows) and a fracture on the SLA brick.

Chemical Compatibility

To create a solvent-resistant barrier, we coated bricks with a 4 µm layer of Parylene-C (Di-chloro-di-p-xylylene; Galentis S.P.A.), which is transparent and used to coat implanted medical devices that hold electronics because it forms a resistant, nonporous ("pinhole-free") barrier to water and a wide range of organic solvents.[33,34] This coating successfully protected bricks from a variety of organic solvents, tested by making contact between the brick and solvent for 5 min, including acetonitrile, dimethyl sulfoxide, tetrahydrofuran, toluene, dichloromethane, N,N-Diisopropylethylamine, hexanes, and dimethylformamide. In contrast, when the coating was removed locally, all of the solvents except the N,N-Diisopropylethylamine and hexanes did immediately discolor and scar the underlying bricks (SI Fig 14 b).

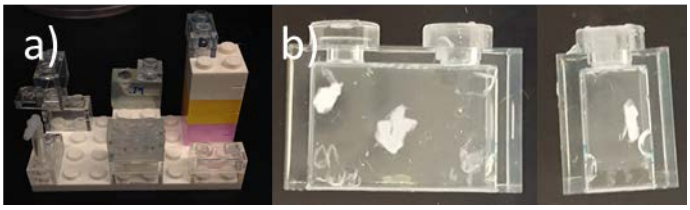

SI Figure 13 (a) Assortment of bricks coated with parylene-C which provides a transparent, solvent-resistant barrier. (b) Coated bricks were unaffected by various organic solvents until the coating was locally scraped off; then, deformation and discoloration were contained within the de-coated areas (*i.e.*, did not leak below the coating).

3D Networks and Larger Bricks

The use of LEGO bricks enables non-planar and extended geometries (SI Fig 15). For example, multiple bricks in combination can create a multiplexed tower to split streams of generated droplets. To fabricate this structure, the bricks were first assembled along with an elastomeric seal between each layer, and then the assembly was machined with the path. The block assembly was covered with a single polyethylene sheet over the front surface so that O-rings were not necessary.

In addition, we can use longer bricks for processes like mixing fluids and generating droplets when we would also like further space to analyze the mixing or reactions.

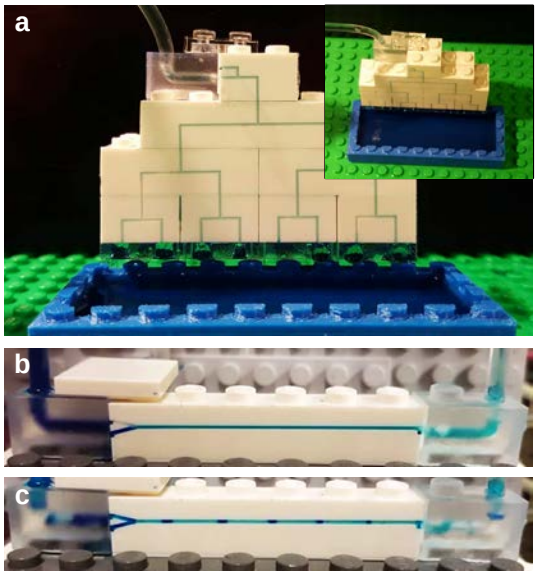

SI Fig 14. (a) A 3-dimensional system for multiplexed production of droplets, which are ejected and collected in a 3D-printed bath below the system. (b) Laminar flow and (c) droplet generation shown through the length of long bricks.